East European Journal of Physics. 1. 342-354 (2024)
DOI:10.26565/2312-4334-2024-1-32 ISSN 2312-4334

SYNTHESIS, CHARACTERIZATION AND FUNCTIONALIZATION OF P3HT-CNT NANOCOMPOSITE THIN FILMS WITH DOPED Ag_2O

Hayder Abdulmeer Abbas[a]*, Wissem Cheikrohou Koubaa[b], Estabraq Talib Abdullah[c]
[a]*Middle Technical University, Technical Instructor Training Institute, Baghdad, Iraq*
[b]*University of Sfax, Faculty of Science of Sfax, Tunisia*
[c]*University of Baghdad College of Science, Department of Physics, Iraq*
**Corresponding Author e-mail: hayder@mtu.edu.iq: Tel.: +964 771 407 3394*
Received December 7, 2023; revised December 29, 2023; accepted January 11, 2023

This research focuses on the synthesis of carbon nanotube (CNT) and Poly(3-hexylthiophene) (P_3HT) (pristine polymer) with Ag doped (CNT/ P_3HT@Ag) nanocomposite thin films to be utilised in various practical applications. First, four samples of CNT solution and different ratios of the polymer (P_3HT) [0.1, 0.3, 0.5, and 0.7 wt.%] are prepared to form thin layer of P_3HT@CNT nanocomposites by dip-coating method of Ag. To investigate the absorption and conductivity properties for use in various practical applications, structure, morphology, optical, and photoluminescence properties of CNT/P_3HT @Ag nanocomposite are systematically evaluated in this study. In this regard, the UV/Vis/NIR spectrophotometer in the wavelength range of 350 to 700 nm is used to investigate the absorption, transmission spectrum, extinction coefficient (k) and refractive index of the samples prepared at room temperature. The XRD results indicate a slight increase in the crystallite size of the synthesized (CNT/ P_3HT@Ag) nanocomposite compared to CNT/P_3HT nanocomposite, which can be attributed to the better dispersion of the P_3HT and its favorable wrapping around the carbon nanotube structures. FESEM results show that the Ag nanoparticles are acting as a bridge between the CNT and P_3HT, creating a strong bond between the two materials that is strong enough to form thicker tubular structures. An appreciable increase in absorbance intensity (approximately 552 nm) is obtained by adding silver nanoparticles to the CNT/P3HT matrix at 0.5% of P3HT. Additionally, the prepared CNT/P3HT@Ag thin films show greater transmittance – more than 42%, 45%, 49%, and 48% for P3HT concentrations of 1%, 3%, 5%, and 7%, respectively. The preparation of the samples' extinction coefficient (k) and refractive index data show that the inclusion of silver nanoparticles to the CNT/P3HT nanocomposite matrix has a significant improvement over the previous samples (CNT/P3HT composite).
Keywords: *Nanocomposite; Poly(3-hexylthiophene) (P_3HT); Carbon nanotube (CNT) solution; Dip-coating method; Photoluminescence properties; Transmission spectrum*
PACS: 61.46.+w, 78.55.−m, 61.48.De, 11.30.Na

1. INTRODUCTION

Conjugated polymers have attracted a lot of attention lately because they may provide large, lightweight, and reasonably priced solutions. They are very adaptable because they work well with biodegradable and electronic/optoelectronic devices such organic solar cells, field effect transistors, and organic light emitting diodes [1]. That being said, most of these devices perform worse than more conventional mining methods. This is because conjugated polymers have a lot of imperfections poor mechanical qualities, and low stability [2]. In order to address these problems, the scientists investigated the application of inorganic nanoparticles/quantum dots and conductive polymers as nanocomposite materials in the creation of organic devices [3, 4].

Semiconductors with low processing costs, simple production processes, flexibility, and high operational power show promise for use in next optical devices. Due to the mid-conductor's comparatively high adsorption coefficient, these semiconductors allow for effective light absorption in thin films, paving the way for more sophisticated optoelectronic device applications [5].

The use of Poly(3-hexylthiophene) (P3HT) as the active layer in different organic devices in conjunction with specific n-type semiconductors has been the subject of extensive research over the last several years. P3HT is a highly desirable conjugated polymer due to its ability to easily dissolve in various solvents, making it an ideal candidate for processing as a soluble solid. With a high band gap of 1.9 electrons, it is well-suited for absorbing powerful sunlight, which in turn promotes the absorption of solar light. Moreover, its high cavity mobility makes it particularly attractive for use in developing organic semiconductor devices [6]. Despite its advantageous solubility and high band gap, P3HT's low conductivity, instability, and short transmission range, make it less suitable for electronic devices compared to inorganic materials [7]. To allow P3HT to be used in electrical devices, these issues need to be addressed. In the polymer matrix, it should be noted that the arrangement of the chain is closely linked to the conductivity and optical properties of the conjugated π-conductors.

The mineral composition, which possesses higher momentum compared to its organic counterparts, has been extensively researched in order to enhance the physical properties of the ahadist. Carbon-based nanomaterials such as multi-walled carbon nanotubes (MWCNT), graphene, and fullerenes are being thoroughly examined as potential filler materials that could lead to improved physical properties [8]. In this regard, carbon nanotubes (CNTs) are widely used in various semiconductor devices as electrodes, semiconductors, transparent electrodes, gas sensors, etc. due to their high

Cite as: H.A. Abbas, W.C. Koubaa, E.T. Abdullah, East Eur. J. Phys. 1, 342 (2024), https://doi.org/10.26565/2312-4334-2024-1-32

conductivity, high surface area, low mass density, and carrier mobility [9]. However, depositing a uniform thin layer of MWCNTs can be challenging, as they are chemically inert and insoluble in most solvents. Previous studies have shown that incorporating carbon-based nanomaterials can enhance the field-effect mobility. Nanocomposites based on nanoparticles indicated an improved performance in solar cells, LEDs, thermoelectric devices, and thin-film transistors (TFTs) [10-12].

Polymer composites are created by synthesizing polymers with nanoparticles, which helps to enhance their electronic and optical properties. CNTs are particularly promising materials for the fabrication of CNT/CNT composites because of their desirable characteristics, including high mechanical strength, high electrical conductivity, adjustable work performance, and soluble processing ability [13].

Photovoltaic cells and other electronic device applications are among the many applications for which polymer compositions containing carbon nanotubes offer tremendous potential. Additionally, achieving balanced injection and transfer for both types of carriers is crucial for the effective functioning of the system, and carbon nanotubes' high electron mobility plays a major part in this regard [6]. This performance can be improved even further by aligning the CNTs [14]. For example, the electric field at the polymer-CNT interface can promote de-oxidization and act as an electrical conduit to improve the charge and direction of light [15]. Due to their ease of processing, MWCNTs are more economical to create than their single-walled counterparts (SWCNTs) [16]. MWCNTs offer greater mechanical strength for composite-based systems and are more suitable for carrier transport than SWCNTs.

Rathore et al. [6] suggested the integration of P3HT with CNTs to form a CNT/polymer composite to overcome the issues of P3HT. They demonstrated that adding MWCNTs to the polymer matrix enhances the current density and modifies the absorption properties of the device.

Conducting polymers (CPs) have gained attention in the field of organic electronics due to their various advantages, such as ease of preparation in thin layers and the ability to adjust their band gap through chemical methods. CPs have been employed in various applications, including organic light emitting diodes (OLEDs), organic gas sensors (OGS), and organic solar cells (OSCs) [15, 16-20]. Among these CPs, P3HT is commonly used in OGSs and OSCs because it has a relatively narrow energy band of 1.93-1.95 eV, [21] allowing it to absorb a broad spectrum of solar energy.

As per the information provided, conjugated polymer materials have gained the interest of both scientists and engineers due to their ability to exhibit electrical and optical properties similar to semiconductors or metals, while also maintaining desirable mechanical properties and processing advantages of polymers. Soon after their discovery, these materials were recognized as potential candidates for use in electronic devices, including cost-effective alternatives for traditional LEDs, photovoltaic cells, and even disposable electronic devices. Poly(alkylthiophene), specifically poly(3-hexylthiophene) or P3HT, is significant because of its high chemical stability under various environmental conditions, high conductivity, and electronic gap that typically falls within the visible range of the electromagnetic spectrum [22-24].

Over the past few years, the preparation of thin films of P3HT, specifically rrP3HT, through solution processing has become increasingly important for various applications such as photovoltaic cells and field effect transistors. Researchers ascertained that the optoelectronic properties of P3HT films are affected by the microstructure and morphology of the prepared film. Generally, CNTs possess an appropriate structure that can interact with conjugated polymers via π-π electronic interactions. The conductive nanocomposites demonstrated that CNTs are an excellent choice for enhancing the optoelectronic properties of conjugated polymers. Specifically, fillers with an aspect ratio of 10^3, such as SWNTs, can potentially result in a penetration threshold of less than 1% by weight. In this regard, Baibarac et al. [25] focused on composites containing MWNTs and conjugated polymers, particularly poly(phenylene vinylene) derivatives. They showed that there are interactions between the polymer and the outermost walls of the nanotube base plate.

Poly(3-hexylthiophene-2,5-diyl) (P3HT) is commonly employed as a light-absorbing material and as a hole transporting layer [26], as it exhibits a high level of molecular order through π-π stacking of neighboring molecules. When CNTs are introduced into P3HT-based organic photovoltaic devices, they have been found to enhance the dissociation rate of excitons and improve the efficiency of charge carrier collection.

Sa'aya et al. [27] and Nguyen [28] indicated that the process of producing films using conjugated polymers and CNTs would result in a greater degree of miscibility due to strong Van der Waals interactions between conjugated π bonds.

Up to the authors' knowledge, the structural characteristics of CNT/P3HT and Ag doped-CNT/P3HT nanocomposites have not been yet investigated in the open loyetature. Thus, this study comes to fill this gap. The main aim is to improve the conductivity and absorption of P3HT to be used in a variety of real-world applications. Accordinly, this study intends to synthesise CNT/P3HT and Ag doped-CNT/P3HT nanocomposites thin films. To systematically assure this presumption, the evaluation of the optical, photoluminescent, and structural characteristics of CNT/P3HT and Ag doped-CNT/P3HT (CNT/ P3HT@Ag) nanocomposite thin films are carried out.

2. EXPERIMENTAL PART

2.1. Synthesis steps of P3HT@CNT

In this method, we first soak CNT in ODCB (dichlorobenzene). The amount of CNT is 1g/l, and with a quick calculation, the amount of 0.005 g is needed for 5ml of dichlorobenzene. A dark-colored solution was obtained. In another container, 5g per liter of P3HT was mixed in 5 ml of chloroform. With a quick calculation, this amount is equivalent to 0.025g of P3HT. An orange-colored solution was obtained. Then, the P3HT solution was slowly added to the CNT

solution in 5 steps. To achieve the best result, the dispersing process was achieved for several minutes after each addition. Finally, a dark red solution was obtained. The PET foils were cut and placed on a mild heater. Since the solution has high coloring power and high stickiness, it is slightly toxic and also volatile, and therefore, the foils were covered with a napkin. Then, the solution was spread evenly on the foil with the help of a spray so that an almost uniform surface can be obtained. Four samples were synthesized with CNT: P3HT ratio equal to 0.1, 0.3, 0.5, and 0.7.

2.2. Synthesis of silver oxide

Two grams of silver nitrate were dissolved in twenty-five milliliters of deionized water to create silver oxide. Next, 0.35 g of PVP was dissolved in 75 ml of deionized water to act as a polymerizing agent. It had been assured that the components would dissolve entirely. After adding the silver nitrate solution, the PVP solution was left aside for ten minutes. The solution also received a small addition of sodium hydroxide until its pH reached 10. For one hour, the solution was maintained in a bath that ranged from 70 ºC to 80 ºC until the last sediment formed. After that, the mixture was given to cool fully and the sediment settled for a whole day. The precipitate was dried after the solution had been filtered.

2.3. P3HT@CNT@Ag_2O

The percentage ratio of P3HT to CNT is variable and it was prepared with ratios of 0.1, 0.3, 0.5, and 0.7. To prepare the silver layers, a fixed amount of 0.8 mg was added to the above percentages in the final solution, and it was manually sprayed and dried on the PET substrate.

3. RESULTS AND DISCUSSION

3.1. X-ray diffraction analysis (XRD)

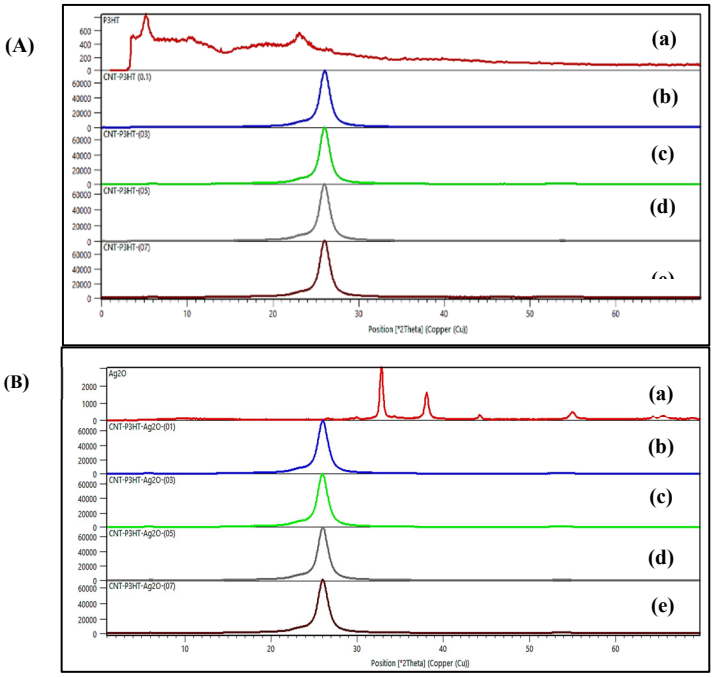

Figure 1. XRD patterns of (A) CNT/P_3HT and (B) CNT/P_3HT@ Ag thin films at different ratios (0.1, 0.3, 0.5, and 0.7 of P_3HT and 0.08 mg/L)

Figure 1 displays the XRD results of the CNT/P_3HT nanocomposite thin films prepared using the dip coating process. In the diffraction spectrum obtained from P_3HT, the scattering peaks at 2θ=5.29° and 23.16° angles were observed, which result from first and higher-order reflections from the large distance large-length d-spacing for this material and are related to the in-plane interchain distance (Figure. 1A-a and Table 1). These reflections show that the polymer chains are arranged regularly and are caused by the material's long-range periodic organization. Higher-order peaks in the diffraction spectrum provide more evidence for this. Stated differently, the material's periodic arrangement produces a diffraction spectrum that displays reflections from the polymer chains as well as additional higher-order peaks that show how the polymer chains are organized. Additionally, the wide-angle peak of the amorphous halo (with less intensity at $2\theta = 23.16°$) reveals the stacking distance between the thiophene rings [29].

Furthermore, it can be stated that by an increase of P_3HT value from 0.1 to 0.3 would cause a slightly amplified in the intensity of the peak [302]. Afterward, peak [302] intensity decreases between 0.3 and 0.5 of P_3HT, which reveals that P_3HT is covering the surface of the CNT, leading to an improved crystallinity. This is especially true for the 0.5 amount of P_3HT, which had the lowest intensity of the [302] peak, indicating the highest level of crystallinity. Also, there is a slight shift in the position of the scattering peaks with the addition of P_3HT to the CNT lattice. The full width at half maximum (FWHM) indicates changes in crystal size values. This can be attributed to the physical wrapping of the polymer on the walls of the nanotubes [29]. Figure 1-B and Table 1 also indicat that the intensity of the [302] peak has been decreased due to adding silver nanoparticles in all cases. In this regard, the lowest peak intensity is at 0.3 P_3HT (Figure 1-B-c), which is also less intense than the previous case (the lowest [302] peak intensity at 0.5 P_3HT (Figure 1-A-d)). This suggests that silver nanoparticles are more effective at reducing [302] peak intensity when the P_3HT concentration in the sample is lower. These findings indicate that silver nanoparticles can therefore have a stronger effect on the [302] peak intensity at lower P_3HT concentrations.

The average crystallite size of the pure structure of P_3HT is about 11 nm, and it is about 6 nm for CNT/P_3HT nanocomposites. This indicates that P_3HT is acting as a template for the CNT to form a more ordered structure, reducing

the size and increasing the crystallinity of the CNT. P_3HT at a 0.5 ratio in CNT/P_3HT nanocomposite reached the highest [302] peak, suggesting a crystalline structure. Also, the average crystallite size of synthesized silver nanoparticles is about 21 nm. By comparing the CNT/P_3HT nanocomposites containing silver nanoparticles (CNT/P_3HT @Ag) compared to their counterparts, a slight increase in the crystallite size can be observed, which can be attributed to the better dispersion of the P_3HT and its favorable wrapping around the carbon nanotube structures. This is because the silver nanoparticles interact with the surface of the carbon nanotubes, forming a stronger bond which aids to stabilize the nanocomposites and prevent the particles from agglomerating. Additionally, the P_3HT forms a protective layer around the particles, further preventing them from agglomerating. The result is a more evenly distributed particles with a larger average crystallite size [29, 30].

Table 1. Parameters obtained from XRD analysis

Sample:	Pos. [°2Th.]	Height [cts]	FWHM [°2Th.]	d-spacing [Å]
P_3HT	5.217	266	0.71	16.92623
CNT/P_3HT (0.1)	26.0593	50259	1.36	3.41664
CNT/P_3HT (0.3)	26.0131	50763	1.322	3.42261
CNT/P_3HT (0.5)	25.9973	43281	1.346	3.4264
CNT/P_3HT (0.7)	26.0179	48557	1.356	3.42198
CNT/P_3HT@Ag (0.1)	26.052	42846	1.296	3.41758
CNT/P_3HT@Ag (0.3)	25.991	41684	1.24	3.41758
CNT/P_3HT@Ag (0.5)	26.0409	42544	1.314	3.41901
CNT/P_3HT@Ag (0.7)	26.0495	42970	1.352	3.411790
Ag_2O	32.836	2084	0.401	2.72535

3.2. Field emission scanning electron microscopy (FESEM) analysis

The FESEM images in Figures 2 and 3 (a), (b), (c), and (d) indicate the morphology of CNT/P_3HT with different ratios of P_3HT (0.1, 0.3, 0.5, 0.7 wt.%) thin films and Ag-doped CNT/ P_3HT (CNT/P_3HT@Ag) nanocomposite thin films (the amount of silver oxide nanoparticles is constant and about 0.08 mg/L), respectively. The FESEM images show a view of CNT nanostructures with polymer wrappings. By comparing the shapes prepared from the samples (from Figure (2-a) to (2-d)), the number of disordered CNT observed has an increasing trend, which is well covered by the desired polymer (P_3HT).

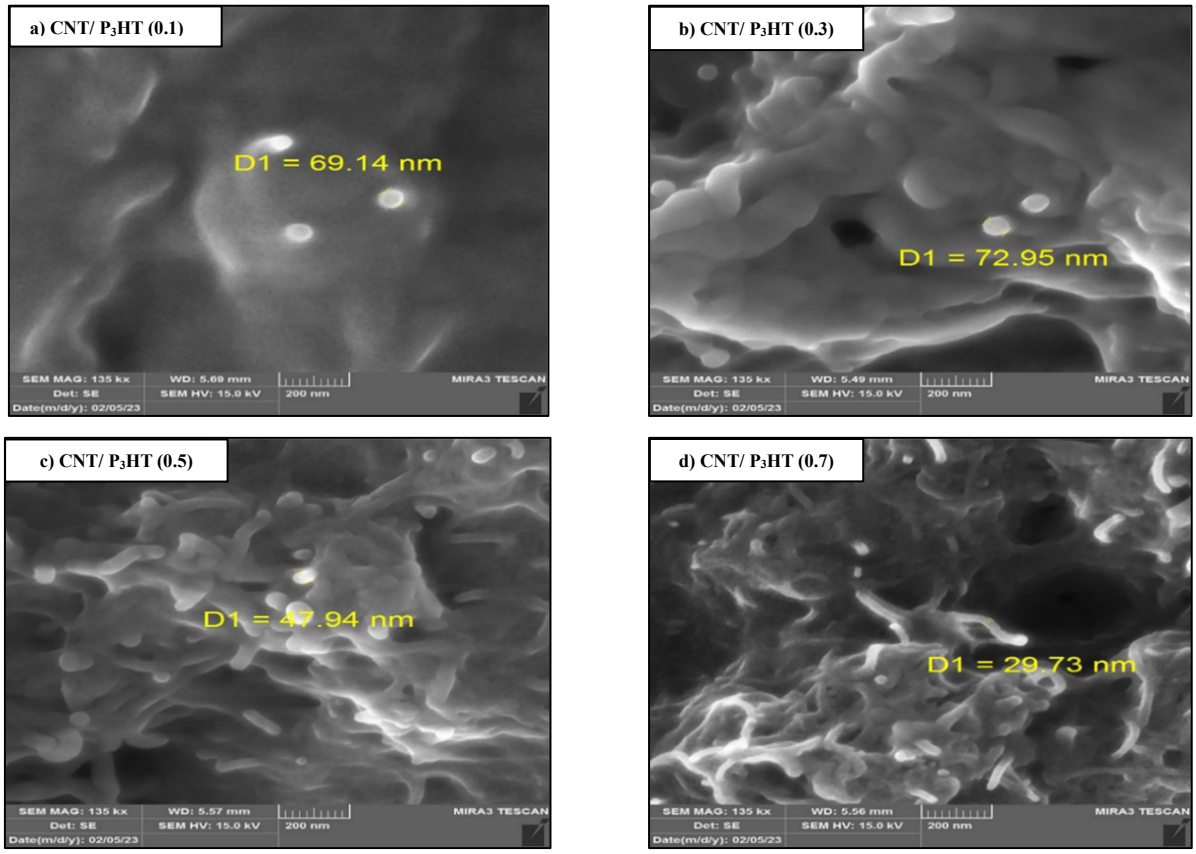

Figure 2. FESEM images of prepared thin films with different P_3HT concentrations: (a) CNT/P_3HT (0.1), (b) CNT/P_3HT (0.3), (c) CNT/P_3HT (0.5), and (d) CNT/P_3HT (0.7)

This is because the polymer matrix can fill in the gaps between CNTs and provide support, leading to an increase in the number of well-buried CNTs in the matrix. This is further evidenced by the FESEM images which show an increasing number of CNTs with tubular structures and well-covered by the polymer matrix. On the other hand, the performance of CNT is still not as impressive as expected due to some factors, including entanglement, misalignment, and metal impurities. These issues can affect the electrical and mechanical properties of CNTs, leading to weaker overall performance. As a result, CNTs cannot reach their full potential and their performance is limited. Based on studies conducted by Danish et al., it can be said that the mentioned issues can lead to a decrease in hole mobility and an increase in recombination pathways [31].

Clearly, Figures (2-a-d) assure that by increasing the amount of P_3HT in the CNT matrix, a more suitable distribution of carbon nanotubes can be achieved. There are, however, still certain regions where entangled nanotubes are visible. This may be due to insufficient amount for P_3HT to overcome the van der Waals forces towards the CNT surface, leading to better dispersion and wrapping. For CNT/P_3HT (0.5 of P_3HT) nanocomposite images in Figure 2-c, less entanglement and improved alignment of CNT can be observed. Also, this Figure shows a completely different surface morphology with an apparently larger CNT diameter. It appears that the exfoliation process has increased the diameter of the CNT due to the presence of newly exfoliated P_3HT chains [32].

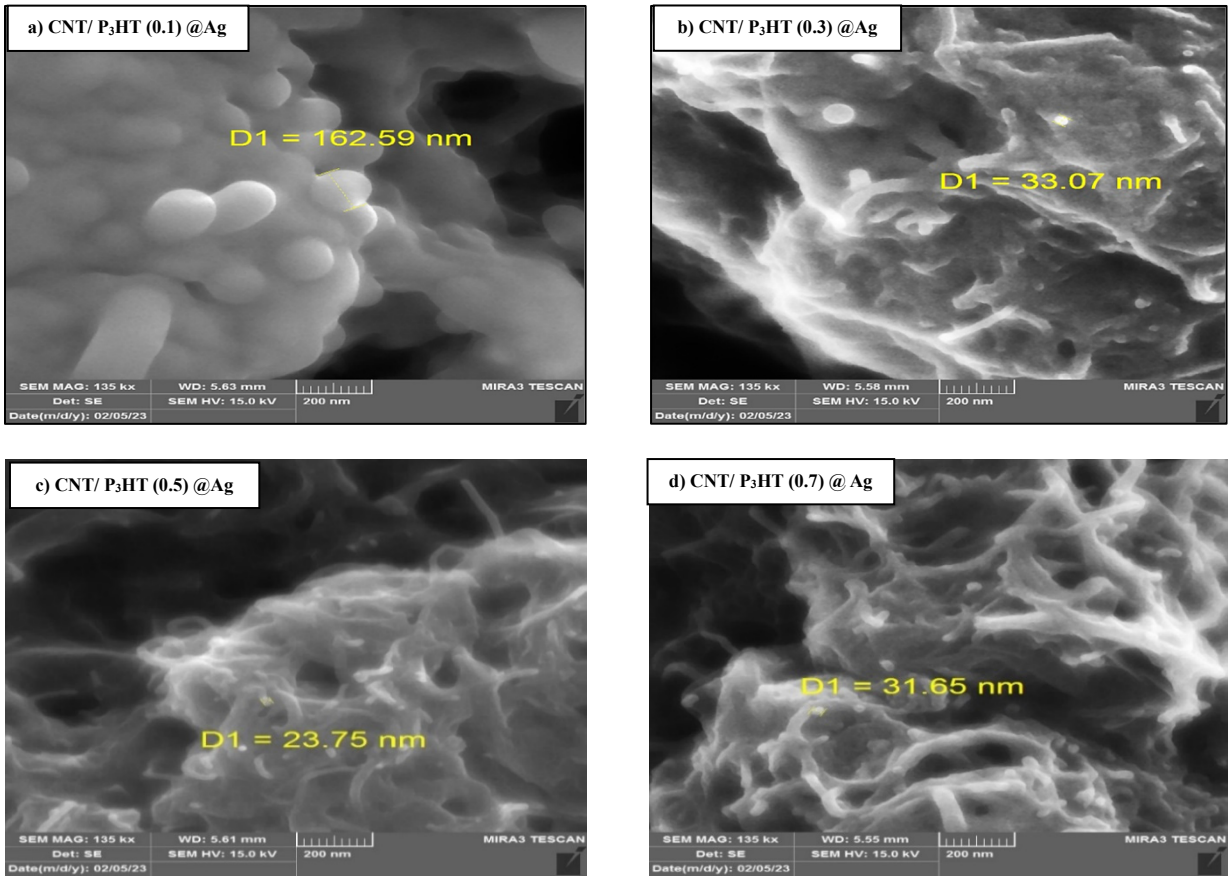

Figure 3. FESEM images of prepared CNT/P_3HT thin films after doping with silver oxide nanoparticles: (a) CNT/P_3HT (0.1)/Ag, (b) CNT/P_3HT (0.3)/Ag, (c) CNT/P_3HT (0.5)/Ag, and (d) CNT/P_3HT (0.7)/Ag [dopant amount: 0.08 mg/L]

The incorporation of silver nanoparticles into the CNT/P_3HT nanocomposite matrix, in smaller amounts of P_3HT (0.3 wt.%) (Figure 3-a-d), can demonstrate a better dispersion and less entanglement for nanotubes. In other words, silver nanoparticles in smaller amounts of P_3HT help the proper dispersion of carbon nanotubes. This is because silver nanoparticles have a strong affinity to the CNT/P_3HT nanocomposite matrix and can act as a bridge between the CNTs and P_3HT, helping to improve alignment and reduce entanglement. Furthermore, the silver nanoparticles reduce the overall viscosity of the nanocomposite matrix, resulting in better dispersion of the CNTs [33]. An average diameter size of the prepared nanocomposites (Figure 2-a-d) continued to decrease from 69 nm, 73 nm, 48 nm to 28 nm. This showed that the increase in the P_3HT concentration reinforces the effectiveness of P_3HT wrapping towards the CNT side-wall by increasing the diameter of CNT [33]. It is also clear from images (3-a-d) that by adding impurity (silver nanoparticles) into the pre-prepared CNT/P_3HT matrix, thicker tubular structures with rough surfaces and agglomerate-like mat structures were obtained, and this illustrates the wrapping of the polymer on the nanotubes to form a nanocomposite [34]. This suggests that the silver nanoparticles are acting as a bridge between the CNT and P_3HT, creating a strong bond between the two materials that is strong enough to form thicker tubular structures. Additionally, the rough surface of the

nanocomposite suggests that the silver nanoparticles are also acting as stabilizing agents to hold the nanotubes and polymer together.

The results of the Electron Diffraction X-ray (EDX) analysis of the CNT/P3HT composite thin films with varying P3HT concentrations (Figure 4-A) show that the carbon content of the composite increases and then decreases, followed by a notable decrease and enhancement in the weight of sulfur (S), indicating the formation of nanocomposites. The EDX analysis data shows that with increasing P_3HT concentration, there is an initial raise in the carbon content of the nanocomposite thin films. This is likely due to the higher content of CNTs in the composite, which contains more carbon than P_3HT. However, after a certain point, the carbon content decreases, indicating that the P3HT is beginning to dominate the composition of the composite. Additionally, the weight of sulfur (S) in the nanocomposite, is reduced and then enhanced, suggesting that there is a chemical interaction between the CNTs and P_3HT in the nanocomposite [29].

Figure 4-B illustrates silver oxide nanoparticles doped successfully in a CNT/P_3HT lattice. This figure demonstrates that adding silver nanoparticles to the pre-prepared nanocomposite lattice leads to the silver oxide nanoparticles forming chemical bonds with the CNTs and P_3HT, further stabilizing the overall nanocomposite lattice. It also suggests that the CNTs and P_3HT facilitate the nanoparticles' dispersal in the nanocomposite lattice. In this regard, Figure 3 obtained from SEM analysis of CNT/P_3HT@Ag nanocomposite thin films confirms the accuracy of these results.

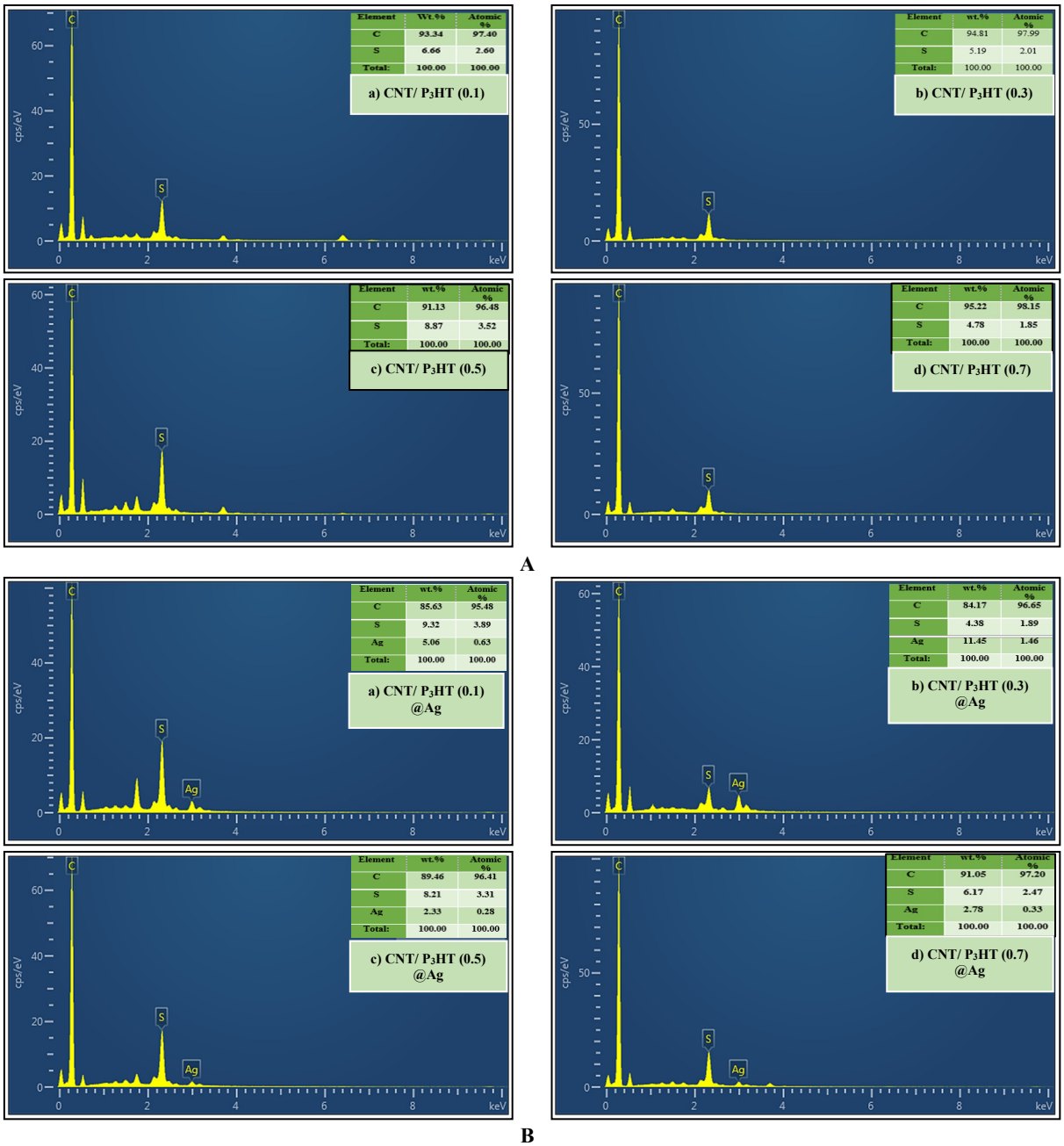

Figure 4. EDX images of (A) CNT/P_3HT thin films with different P_3HT concentrations: (a) CNT/P_3HT (0.1), (b) CNT/P_3HT (0.3), (c) CNT/P_3HT (0.5), and (d) CNT/P_3HT (0.7). EDX (B) CNT/P_3HT thin films after doping with silver oxide nanoparticles: (a) CNT/P_3HT (0.1)/Ag, (b) CNT/P_3HT (0.3)/Ag, (c) CNT/P_3HT (0.5)/Ag, and (d) CNT/P_3HT (0.7)/Ag [dopant amount: 0.08 mg/L]

3.3. Photoluminescence (PL) spectroscopy

Prior to deciding on an appropriate composite composition for uses like photoactive layers, it is important to examine the photoluminescence properties of the pristine polymer (P3HT) and the CNT/P3HT composite thin films. This study is important because the composite that exhibits the strongest quenching of photoluminescence also exhibits the largest charge separation that can be found in the photoactive layer. This is important because the composite film's charge separation potential increases with the strength of the photoluminescence quenching effect. This charge separation is essential to create the desired photoactive layer, which is necessary for the optimal performance of the application [35]. The PL spectrum of the CNT/P_3HT and CNT/P_3HT@Ag nanocomposites measured at an excitation wavelength of 440 nm is presented in Figure 5.

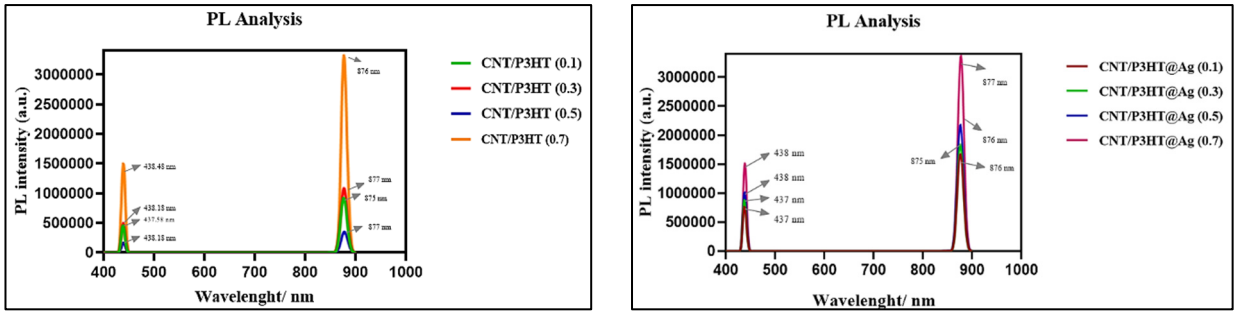

A **B**

Figure 5. PL spectrum of the (A) prepared thin films with different P_3HT concentrations: (a) CNT/P_3HT (0.1), (b) CNT/P_3HT (0.3), (c) CNT/P_3HT (0.5), and (d) CNT/P_3HT (0.7). and (B) CNT/P_3HT thin films after doping with silver oxide nanoparticles: (a) CNT/P_3HT (0.1)/Ag, (b) CNT/P_3HT (0.3)/Ag, (c) CNT/P_3HT (0.5)/Ag, and (d) CNT/P_3HT (0.7)/Ag [dopant amount: 0.08 mg/L]. The excitation wavelength λ = 440 nm

Figure 5-A and 5-B illustrates the values of PL emission for CNT/P_3HT and CNT/P_3HT@Ag nanocomposite for different amounts of P_3HT (0.1, 0.3, 0.5, and 0.7) around 437, 438, 438, and 439 nm and for the CNT/P_3HT@Ag composites around 437, 437, 438, and 438 nm, respectively. Although CNTs are well-known fluorescence quenchers, the physical mixed system between P3HT and CNTs causes photoluminescence quenching to be more noticeable for CNT/P3HT. One other benefit of employing CNT/P3HT in solar cells is this. However, P3HT's emission peak intensity was greater than nanocomposites. This was explained as quenching brought on by the reduction of electron-hole recombination caused by charge transfer between the CNT and P3HT. Strong luminous quenching of the as-prepared nanocomposites was seen at wavelengths of about 876 nm (attributed to the π-π^* bond in P_3HT). According to the reported studies [36, 37], CNTs are known as fluorescence quenchers. However, photoluminescence quenching is expected to be more pronounced for the prepared CNT/P_3HT nanocomposites due to the physical mixed system of P_3HT and CNTs. This phenomenon is an extra benefit for using these systems in photovoltaic applications such as photovoltaic cells [32].

According to these references [35, 38, 39], the emission peak intensity for pure P_3HT is around 581 nm, which is a larger amount compared to the prepared CNT/P_3HT nanocomposites. This behavior can be ascribed to quenching as a result of charge transfer between CNT and P_3HT reducing electron-hole recombination. On the other hand, strong light quenching of the prepared nanocomposites was observed at wavelengths around 876 nm (attributed to the π-π^* bond in P_3HT) [35]. In this regard, Kuila et al. [38] investigated the PL quenching of the CNT/P_3HT nanocomposite and corresponded it to the π-π interaction between the P_3HT and the carbon nanotubes (CNT) and presented additional deactivation (decaying) pathways for excited electrons [37, 39].

As a result, CNT/P_3HT@Ag (0.5 P_3HT) and CNT/P_3HT@Ag (0.1 and then 0.3 P_3HT) quench the PL intensity even more, reducing electron-hole recombination as a result of charge transfer between donor-acceptor materials. With these CNT/P_3HT (0.5 of P_3HT) and CNT/P_3HT@Ag (0.1 of P_3HT) samples, there is a high possibility of charge separation in the photoactive layer due to its strong PL quenching effect [30].

3.4. Ultraviolet-visible (UV-vis) spectroscopy

3.4.1 Absorption spectrum

UV/Vis/NIR spectrophotometer in the wavelength range of 350 to 700 nm was used to investigate the absorption and transmission spectrum of the samples prepared at room temperature. According to Figure 6(a), the absorption spectra of CNT/P_3HT at different ratios (0.1, 0.3, 0.5, and 0.7 wt.%) can be observed.

According to the reference [34], the absorption maximum (λ_{max}) for P_3HT was observed at about 442-505 nm, which indicates extensive π-continuity and is in good agreement with reported values [29]. The CNT/P_3HT composites exhibited absorption bands at about 512-527 nm, which is attributed to the strong interactions between P_3HT and CNTs and suggesting a decrease in band gap [40]. The strong interactions between the two components lead to an increased conjugation of the polymer and the formation of an extended π-conjugated system, which gives rise to the absorption bands in the visible range. Additionally, the intensity of the absorption band raised with increasing P_3HT (0.5 wt.%) concentration, which is due to the enhanced number of P_3HT molecules in the nanocomposite. On the other hand, after

adding silver nanoparticles into the CNT/P_3HT nanocomposite matrix, increasing the percentage of P_3HT to about 0.3, an amplification in the absorption peak intensity is observed; Compared to the previous case, the increase in the amount of absorption intensity is ascertained in lower P_3HT amounts. This suggests that silver nanoparticles play a role in increasing the efficiency of the nanocomposite matrix by allowing for more efficient absorption of light at lower P_3HT percentages. This is due to the expansion of the surface area of the nanocomposite matrix provided by the silver nanoparticles, which allows for more efficient absorption of light [32]. Thus, All CNT/P_3HT samples with different ratios of P_3HT show improved adsorption efficiency. In addition, it is expected to improve electrical conductivity, thereby enhancing the performance of photovoltaic applications [30, 41].

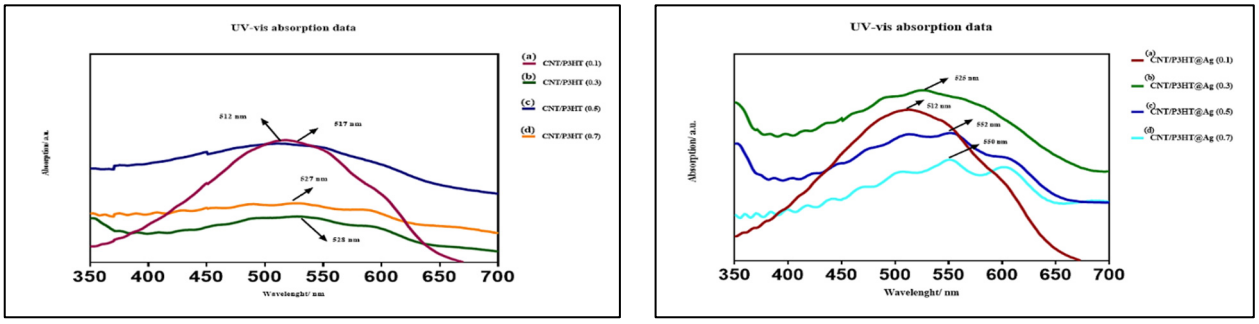

A **B**

Figure 6. Schematic of absorption spectra of (A) prepared thin films with different P_3HT concentrations: (a) CNT/P_3HT (0.1), (b) CNT/P_3HT (0.3), (c) CNT/P_3HT (0.5), and (d) CNT/P_3HT (0.7). and (B) CNT/P_3HT thin films after doping with silver oxide nanoparticles: (a) CNT/P_3HT (0.1)/Ag, (b) CNT/P_3HT (0.3)/Ag, (c) CNT/P_3HT (0.5)/Ag, and (d) CNT/P_3HT (0.7)/Ag [dopant amount: 0.08 mg/L]

But in the case of nanocomposites reinforced with silver nanoparticles (CNT/P_3HT@Ag), as seen in Figure 6-B, a favorable boost in the maximum absorption intensity was observed for all prepared nanocomposite samples compared to pure P_3HT polymer. A significant improvement in absorbance intensity (around 552 nm) is observed when silver nanoparticles are added to the CNT/P_3HT matrix at 0.5% of P_3HT, which is a significant increase compared to the previous samples (CNT/P_3HT composite).

This shift towards longer wavelengths (red-shift of λ_{max}) compared to the CNT/P_3HT nanocomposite matrix as well as the pure P_3HT can be attributed to the enhancement in the conjugation length of the P_3HT polymer due to the strong π-π interaction with CNTs, which subsequently leads to the increased organization of P_3HT chains on the nanotube surface. In the case of silver-reinforced nanocomposites (CNT/P_3HT@Ag), as mentioned earlier, due to the synergistic effect of these nanoparticles, a significant reinforcement in the absorption wavelength can be expected, which is consistent with the results previously obtained [34, 42]. This is because silver nanoparticles can act as a bridge between the P_3HT polymer and the carbon nanotubes, thereby forming a stronger bond that allows for a longer absorption wavelength. This is further reinforced by the fact that silver has a higher optical reflectance than carbon nanotubes, which also contributes to the increased absorption wavelength.

3.4.2. Transmission spectrum

Figure 7-A and 7-B shows the optical transmission spectrum for the as-prepared CNT/P_3HT and CNT/P_3HT@Ag nanocomposite thin films at different P_3HT ratios (0.1, 0.3, 0.5, and 0.7 wt.%) in the wavelength range of 350 to 1000 nm, which is in good agreement with the absorption spectrum data (Figures 7-A and B). Figure 7-A shows the amount of transmission in the visible region for these prepared CNT/P_3HT nanocomposites is more than 20%, 35%, 20%, and 32% for the concentrations of 1%, 3%, 5%, and 7% of P_3HT, which can indicate the good crystal quality of the samples.

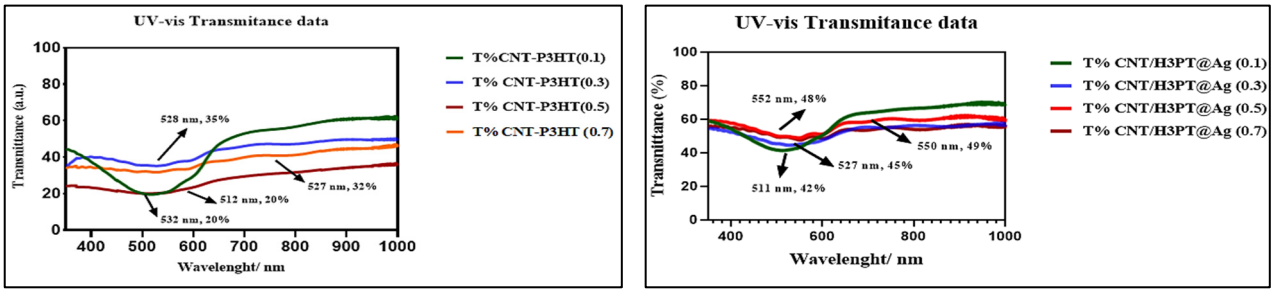

A **B**

Figure 7: Schematic of optical transmission spectra of (A) prepared CNT/P_3HT thin films with different P_3HT concentrations: (0.1), (0.3), (0.5), and (0.7). and (B) CNT/P_3HT thin films after doping with silver oxide nanoparticles: CNT/P_3HT (0.1)/Ag, CNT/P_3HT (0.3)/Ag, CNT/P_3HT (0.5)/Ag, and CNT/P_3HT (0.7)/Ag [dopant amount: 0.08 mg/L]

Also, it is clear from Figure 7-B that the CNT/P_3HT nanocomposite samples have been reinforced with silver nanoparticles (CNT/P_3HT@Ag) with a better transmission spectrum for all P_3HT concentrations (0.1, 0.3, 0.5, and 0.7 wt.% of P_3HT). In other words, the amount of transmittance in the visible region for the as-prepared CNT/P_3HT@Ag thin films, in this case, is more than 42%, 45%, 49%, and 48% for the concentrations of 1%, 3%, 5%, and 7% of P_3HT, which can indicate the synergistic effect caused by the integration of silver nanoparticles in the CNT/P_3HT nanocomposite matrix. The silver nanoparticles enhance the light absorption and scattering of the nanocomposite matrix, which increases the amount of light transmitted in the visible region. This improves the light transmission results in higher transmittance values for the CNT/P_3HT@Ag thin films than for pure CNT/P_3HT thin films.

3.4.3. Absorption coefficient

By knowing the data of the transmission spectrum of the CNT/P_3HT and CNT/P_3HT@Ag nanocomposites at different P_3HT ratios (0.1, 0.3, 0.5, and 0.7 wt.%) (Figure 7), it is possible to calculate the absorption coefficient (8-A/B) of the as-prepared nanocomposites. The result of these calculations regarding the absorption coefficient spectrum of the samples as a function of wavelength. As can be seen from Figure 8-A, at long wavelengths (greater than 600 nm) there is very small absorption (all photons are transmitted), and at shorter wavelengths, i.e., at wavelengths between 510-528 nm, the absorption has the highest value (in the range of 0.0115-0.0164). It is expected that in this area, the transmission value in this range will decrease due to the transition of electrons from the valence band to the conduction band. This is in a reasonable agreement with the data obtained from the transmission spectrum (Figure 8-A). Specifically, the decrease in transmission value is due to the fact that when electrons transit from the valence band to the conduction band, their energy is absorbed. This energy is converted into heat, which reduces the ability of the material to transmit light. This decrease in the transmission is further evidenced by the transmission spectrum in Figure 8-A, which shows a decrease in intensity in the range of interest.

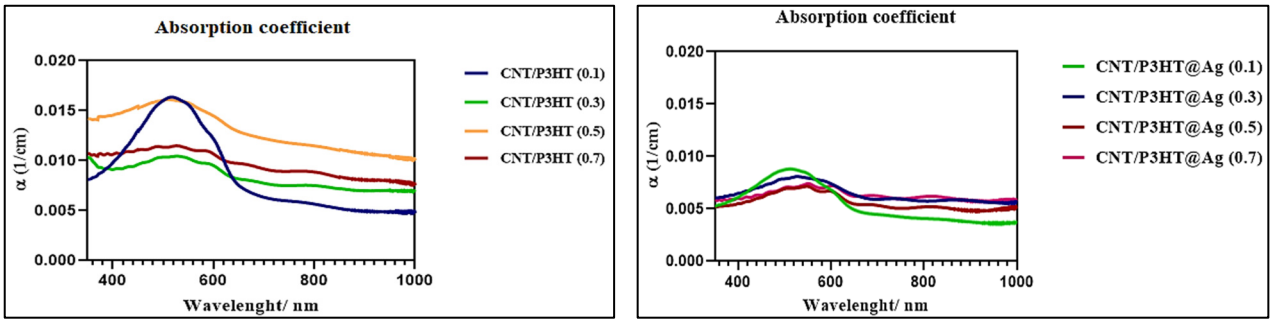

A **B**

Figure 8. Schematic of absorption coefficient of (A) prepared thin films with different P_3HT concentrations: (0.1), (0.3), (0.5), and (0.7). and (B) CNT/P_3HT thin films after doping with silver oxide nanoparticles: CNT/P_3HT (0.1)/Ag, CNT/P_3HT (0.3)/Ag, CNT/P_3HT (0.5)/Ag, and CNT/P_3HT (0.7)/Ag [dopant amount: 0.08 mg/L]

Also, as can be seen from Figure 8-B, at long wavelengths (greater than 640 nm) there is very small absorption (most photons are transmitted), and at shorter wavelengths, i.e., at wavelengths between 512-600 nm, the absorption has the highest value (in the range of 0.0072-0.0088), which is in reasonable agreement with the data obtained from the transmission spectrum (Figure 7-B). The data related to the maximum absorption coefficient and the wavelength at which the absorption coefficient has its maximum value are presented in Table 2.

In addition, by comparing the absorption coefficient data for CNT/P_3HT and CNT/P_3HT@Ag nanocomposites, it can be seen that CNT/P_3HT nanocomposites have been reinforced with silver nanoparticles (CNT/P_3HT@Ag) as they have a lower absorption coefficient than their counterparts (CNT/P_3HT). However, it should be noted that the maximum absorption coefficient occurs for CNT/P_3HT@Ag nanocomposites at different wavelengths (shift towards larger wavelengths) compared to CNT/P_3HT thin films.

Table 2. Wavelength of peaks and their maximum absorption coefficient of as-prepared CNT/P_3HT and CNT/P_3HT/Ag nanocomposite thin films

Samples		Wavelength of peaks and their maximum absorption coefficient			
		P_3HT (0.1)	P_3HT (0.3)	P_3HT (0.5)	P_3HT (0.7)
CNT/P_3HT	λ(nm)	517	528	510	527
	α_{max}	0.016	0.0146	0.016	0.0115
CNT/P_3HT@Ag	λ (nm)	512	527	547	600
	α_{max}	0.0088	0.0081	0.0071	0.0072

3.4.4. Extinction coefficient (K)

With the help of the absorption coefficient and absorption data, the extinction coefficient (k) of CNT/P_3HT and CNT/P_3HT@Ag nanocomposites can be found. The changes in k in terms of λ are plotted in Figure 9 for these samples. According to these graphs (Figure 9- A-a to d), the extinction coefficient of CNT/P_3HT nanocomposites at different P_3HT ratios (0.1, 0.3, 0.5, and 0.7 wt.%) with increasing wavelength first has a peak in the areas (545 nm, 1005 nm, 1011 nm, and 993 nm) and then starts to decrease and is almost constant at long wavelengths. It should be noted that this rate of reduction is rapid only for CNT/P_3HT containing 0.1 wt.% of P_3HT, and it decreases slowly for the remaining three samples. The reason for the decrease in the extinction coefficient with the increase in wavelength is related to the decrease in absorption in the thin films, which corresponds to the optical transmission spectrum of the samples in Figure 7. Also, for the CNT/P_3HT nanocomposite reinforced with silver nanoparticles (CNT/P_3HT@Ag), a similar trend was observed. With the difference owing to the sample containing 0.1 of P_3HT, the decreasing trend compared to its counterpart (Figure 9-A), has a slower rate. According to these graphs (Figure 9-B), the extinction coefficient of CNT/P_3HT@Ag nanocomposites at different P_3HT ratios (0.1, 0.3, 0.5, and 0.7 wt.%) with increasing wavelength first has a peak in the areas (545-1005 nm) and then starts to decline with an almost constant and similar reduction rate and is almost constant at long wavelengths.

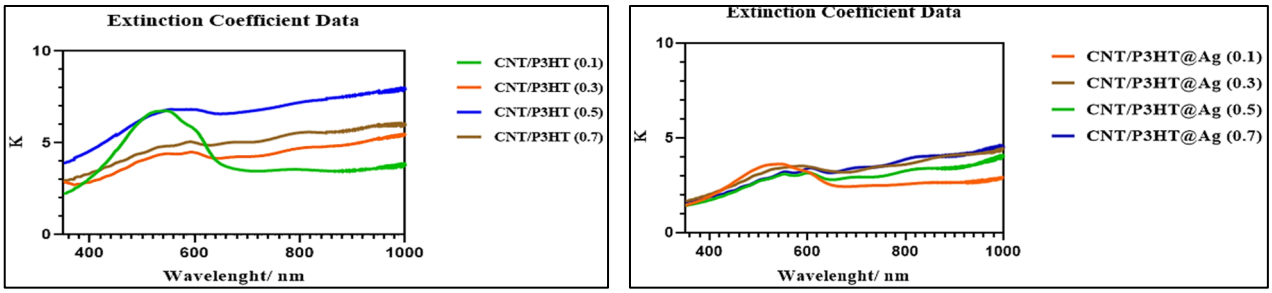

A **B**

Figure 9. Variations in extinction coefficient according to wavelength for (A) CNT/P_3HT and (B) CNT/P_3HT@Ag nanocomposites with different P_3HT ratios

3.4.5. Refractive index (n)

Based on the data obtained from the optical analysis, the refractive index of CNT/P_3HT and CNT/P_3HT@Ag nanocomposites can be obtained. Figure 10-A/B shows the change in the refractive index according to the wavelength of the prepared samples. In other words, the refractive index of CNT/P_3HT and CNT/P_3HT@Ag nanocomposites decreases with increasing wavelengths. By comparing Figures 10-A and B, only the samples containing 0.1% of P_3HT have a significant decrease in the refractive index, which occurs at the wavelengths of 517 nm and 512 nm for CNT/P_3HT and CNT/P_3HT@Ag nanocomposites, respectively. But for the other three samples, a slight decrease in the refractive index can be observed. Finally, the refractive index reaches an almost constant value for all samples with increasing wavelengths. Also, Table 3 illustrates the wavelength of peaks and their minimum reflective index of as-prepared CNT/P_3HT and CNT/P_3HT@Ag nanocomposite thin films.

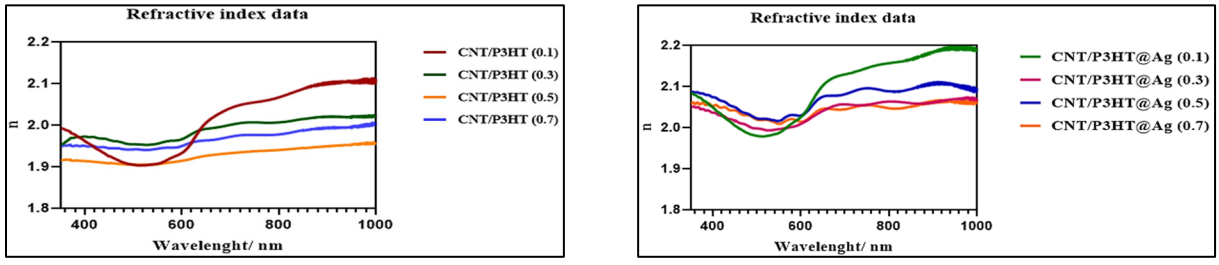

A **B**

Figure 10. Variations in reflective index according to wavelength for (A) CNT/P_3HT and (B) CNT/P_3HT@Ag nanocomposites with different P_3HT ratios

Table 3. Wavelength of peaks and their minimum reflective index of as-prepared CNT/P_3HT and CNT/P_3HT/Ag nanocomposite thin films

Samples		Wavelength of peaks and their minimum reflective index			
		P_3HT (0.1)	P_3HT (0.3)	P_3HT (0.5)	P_3HT (0.7)
CNT/P_3HT	λ(nm)	517	526	512	490
	n_{min}	1.902	1.953	1.904	1.941
CNT/P_3HT@Ag	λ (nm)	512	527	547	550
	n_{min}	1.978	1.993	2.015	2.009

CONCLUSIONS

This study reported on the structure, morphology, optical, and photoluminescence properties of CNT/P3HT and Ag doped-CNT/P3HT (CNT/ P3HT@Ag) nanocomposite thin films synthesised by dip-coating method. The study intended to enhance P3HT absorption and conductivity properties for use in various practical applications and systematically the effects on the structure, morphology, optical and photoluminescence were investigated. The XRD results exhibited the average crystallite size of synthesized silver nanoparticles is about 21 nm. By comparing the CNT/P3HT nanocomposites containing silver nanoparticles (CNT/P3HT @Ag) compared to their counterparts, a slight increase in the crystallite size was observed, which can be attributed to the better dispersion of the P3HT and its favorable wrapping around the carbon nanotube structures. The FESEM results showed that the silver nanoparticles are acting as a bridge between the CNT and P3HT, creating a strong bond between the two materials that is strong enough to form thicker tubular structures. The photoluminescence characteristics of both the pristine polymer (P_3HT) and the CNT/P_3HT composite thin films ascertained that adding silver nanoparticles to the CNT/P3HT matrix at 0.5% of P3HT results in a notable rise in absorbance intensity (about 552 nm), which is a considerable improvement over the prior samples (CNT/P3HT composite). Also, when silver nanoparticles are integrated into the CNT/P3HT nanocomposite matrix, the as-prepared CNT/P3HT@Ag thin films exhibit more transmittance—more than 42%, 45%, 49%, and 48% for P3HT concentrations of 1%, 3%, 5%, and 7%, respectively. Finally, the results of extinction coefficient (k) and refractive index of the samples prepared at room temperature have demonstrated that the addition of silver nanoparticles to the CNT/P3HT nanocomposite matrix has a synergistic impact.

Funding.
This research received no external funding.

Conflicts of Interest.
The authors declare no conflict of interest.

Data availability statement.
The data that support the findings of this study are available from the corresponding author upon reasonable request.

ORCID

Hayder Abdulmeer Abbas, https://orcid.org/0009-0002-1029-2353
Wissem Cheikrohou Koubaa, https://orcid.org/0000-0001-8907-0379
Estabraq Talib Abdullah, https://orcid.org/0000-0002-2893-3529

REFERENCES

[1] S. Shi, S. Ravi, and P. Silva, "High luminance organic light-emitting diodes with efficient multi-walled carbon nanotube hole injectors," Carbon, **50**, 4163-4170 (2012). https://doi.org/10.1016/j.carbon.2012.04.065
[2] A.K. Singh, and R. Prakash, "Organic Schottky diode based on conducting polymer nanoclay composite," RSC Advances, **2**, 5277-5283 (2012). https://doi.org/10.1039/C2RA20206A
[3] A. Bruno, T.D. Luccio, C. Borriella, F. Villani, S. Haque, and C. Minarini, "Exciton dynamics in hybrid polymer/qd blends," Energy Procedia, **44**, 167-175 (2014). https://doi.org/10.1016/j.egypro.2013.12.024
[4] S. Lee, B.R. Lee, J. Kim, and M.H. Song, "Combination effect of polar solvent treatment on ZnO and polyuorene-based polymer blends for highly efficient blue based hybrid organic inorganic polymer light-emitting diodes," Journal of Materials Chemistry C, **2**, 8673-8677 (2014). https://doi.org/10.1039/C4TC01726A
[5] J. Shi, J. Zhang, L. Yang, M. Qu, D.C. Qi, and K.H. Zhang, "Wide bandgap oxide semiconductors: from materials physics to optoelectronic devices," Advanced materials, **33**(50), 2006230 (2021). https://doi.org/10.1002/adma.202006230
[6] P. Rathore, C.M.S. Negi, A.S. Verma, A. Singh, G. Chauhan, A.R. Inigo, and S.K. Gupta, "Investigation of the optical and electrical characteristics of solution-processed poly (3 hexylthiophene) (P3HT): multiwall carbon nanotube (MWCNT) composite-based devices," Materials Research Express, **4**(8), 085905 (2017). https://doi.org/10.1088/2053-1591/aa7dac
[7] R. Meitzner, T. Faber, S. Alam, A. Amand, R. Roesch, M. Büttner, F. Herrmann-Westendorf, et al., "Impact of P3HT materials properties and layer architecture on OPV device stability," Solar Energy Materials and Solar Cells, **202**, 110151 (2019). https://doi.org/10.1016/j.solmat.2019.110151
[8] N. Rao, R. Singh, and L. Bashambu, "Carbon-based nanomaterials: Synthesis and prospective applications," Materials Today: Proceedings, **44**, 608-614 (2021). https://doi.org/10.1016/j.matpr.2020.10.593
[9] W. Aloui, A. Ltaief, and A. Bouazizi, 2013. Transparent and conductive multi walled carbon nanotubes flexible electrodes for optoelectronic applications. Superlattices and Microstructures, 64, 581-589.
[10] P.C. Mahakul, and P. Mahanandia, "Structural and electrical characteristics of solution processed P3HT-carbon nanotube composite," IOP Conference Series: Materials Science and Engineering, **178**(1), 012024 (2017). https://doi.org/10.1088/1757-899X/178/1/012024
[11] Q.A. Yousif, K.M. Mahdi, and H.A., Alshamsi, "Enhanced photovoltaic performance of dye-sensitized solar cell based on ZnO nanoparticles and ZnO/graphene nanocomposites," Journal of the Chinese Chemical Society, **68**(9), 1637-1643 (2021). https://doi.org/10.1002/jccs.202000382
[12] F. Ziaeifar, A. Alizadeh, and Z. Shariatinia, "Dye sensitized solar cells fabricated based on nanocomposite photoanodes of TiO_2 and $AlMo_{0.5}O_3$ perovskite nanoparticles," Solar Energy, **218**, 435-444 (2021). https://doi.org/10.1016/j.solener.2021.03.024
[13] H-J. Hwang, S-J. Joo, and H-S. Kim, "Copper nanoparticle/multiwalled carbon nanotube composite films with high electrical conductivity and fatigue resistance fabricated via flash light sintering," ACS Applied Materials Interfaces, **7**, 25413-25423 (2015). https://doi.org/10.1021/acsami.5b08112

[14] B. King, and B. Panchapakesan, "Vacuum filtration-based formation of liquid crystal films of semiconducting carbon nanotubes and high-performance transistor devices," Nanotechnology, **25**, 175201 (2014). https://doi.org/10.1088/0957-4484/25/17/175201
[15] M. Zhang, S. Höfle, J. Czolk, A. Mertens, and A. Colsmann, "All-Solution Processed Transparent Organic Light Emitting Diodes," Nanoscale, **7**, 20009-20014 (2015). https://doi.org/10.1039/C5NR05820A
[16] W. Zhou, X. Bai, E. Wang, and S. Xie, "Synthesis, structure, and properties of single-walled carbon nanotubes," Advanced Materials, **21**(45), 4565-4583 (2009). https://doi.org/10.1002/adma.200901071
[17] D. Luo, Q.B. Chen, B. Liu, and Y. Qiu, "Emergence of Flexible White Organic Light-Emitting Diodes," Polymers, **11**, 384 (2019). https://doi.org/10.3390/polym11020384
[18] G. Li, R. Zhu, and Y. Yang, "Polymer Solar Cells," Nature Photonics, **6**, 153-161 (2012). https://doi.org/10.1038/nphoton.2012.11
[19] Y.Y. Gao, Z. Wang, G.T. Yue, X. Yu, X.S. Liu, G. Yang, F.R. Tan, et al., "Efficient Polymer Solar Cells with High Fill Factor Enabled by a Furo[3,4-c] Pyrrole-4,6-Dione-Based Copolymer," Solar RRL, **3**, 1900012 (2019). https://doi.org/10.1002/solr.201900012
[20] Z.J. Zhang, J.H. Miao, Z.C. Ding, B. Kan, B.J. Lin, X.J. Wan, W. Ma, et al., "Efficient and Thermally Stable Organic Solar Cells Based on Small Molecule Donor and Polymer Acceptor," Nature Communications, **10**, 3271 (2019). https://doi.org/10.1038/s41467-019-10984-6
[21] S. Ren, L.Y. Chang, S.K. Lim, J. Zhao, M., Smith, N. Zhao, V. Bulovic, et al., "Inorganic Organic Hybrid Solar Cell: Bridging Quantum Dots to Conjugate Polymer Nanowire," Nano Letters, **11**, 3998-4002 (2011). https://doi.org/10.1021/nl202435t
[22] D. Chaudhary, S. Munjal, N. Khare, and V.D. Vankar, "Bipolar resistive switching and nonvolatile memory effect in poly (3-hexylthiophene)–carbon nanotube composite films," Carbon, **130**, 553-558 (2018). https://doi.org/10.1016/j.carbon.2018.01.058
[23] M.D. Hampton, "Polythiophene nanowires for use in organic electronic applications," PhD diss, Cardiff University, 2012.
[24] M. Tonga, "A Rational Ternary Design of P3HT/Insulating Polymers–CNTs/P3HT for the Enhanced Thermoelectric Performances," Composite Interfaces, **29**(2), 197-213 (2022). https://doi.org/10.1080/09276440.2021.1913900
[25] M. Baibarac, G. Arzumanyan, M. Daescu, A. Udrescu, and K. Mamatkulov, "Anisotropic Photoluminescence of Poly (3-hexyl thiophene) and Their Composites with Single-Walled Carbon Nanotubes Highly Separated in Metallic and Semiconducting Tubes," Molecules, **26**(2), 294 (2021). https://doi.org/10.3390/molecules26020294
[26] H. Zhu, M. Pan, M.B. Johansson, and E.M. Johansson, "High photon-to-current conversion in solar cells based on light-absorbing silver bismuth iodide," ChemSusChem, **10**(12), 2592-2596 (2017). https://doi.org/10.1002/cssc.201700634
[27] N.S.N. Sa'aya, S.Z.N. Demon, N. Abdullah, A. Shatar, V.F.K. Ernest, and N.A. Halim, "Optical and Morphological Studies of Multiwalled Carbon Nanotube-incorporated Poly (3-hexylthiophene-2, 5-diyl) Nanocomposites," Sensors & Materials, **31**, 2997-3006 (2019). https://doi.org/10.18494/SAM.2019.2513
[28] P.H.N. Nguyen, "Facile preparation, characterization of flexible organic solar cells using P3HT-MWCNTs composite photoactive layer," Journal of Materials Science and Chemical Engineering, **8**, 1-10 (2020). https://doi.org/10.4236/msce.2020.810001
[29] M.R. Karim, "Synthesis and characterizations of poly (3-hexylthiophene) and modified carbon nanotube composites," Journal of Nanomaterials, **2012**, 34-38 (2012). https://doi.org/10.1155/2012/174353
[30] S. Qotso, P. Mbule, and B. Mothudi, "Characterization of P3HT-CNT thin films for photovoltaic solar cell applications," in: *SAIP 2021 Proceedings*, https://events.saip.org.za/event/206/contributions/7086/contribution.pdf
[31] D. Khan, et al., "Incorporation of carbon nanotubes in photoactive layer of organic solar cells," Ain Shams Engineering Journal, **12**(1), 897-900 (2021). https://doi.org/10.1016/j.asej.2020.06.002
[32] B.K. Kuila, K. Park, and L. Dai, "Soluble P3HT-grafted carbon nanotubes: synthesis and photovoltaic application," Macromolecules, **43**(16), 6699-6705 (2010). https://doi.org/10.1021/ma100917p
[33] N. Nurazzi, N. Abdullah, S.Z.N. Demon, N.A. Halim, and I.S. Mohamad, "The Influence of Reaction Time on Non-Covalent Functionalisation of P3HT/MWCNT Nanocomposites," Polymers, **13**(12), 1916 (2021). https://doi.org/10.3390/polym13121916
[34] G. Keru, P.G. Ndungu, G.T. Mola, and V.O. Nyamori, "Bulk heterojunction solar cell with nitrogen-doped carbon nanotubes in the active layer: effect of nanocomposite synthesis technique on photovoltaic properties," Materials, **8**(5), 2415-2432 (2015). https://doi.org/10.3390/ma8052415
[35] T.S.T. Khanh, N.P.H. Nam, and N.N. Dinh, "Facile preparation, characterization of flexible organic solar cells using P3HT-MWCNTs composite photoactive layer," Journal of Materials Science and Chemical Engineering, **8**, 1-10 2020. https://eprints.uet.vnu.edu.vn/eprints/id/eprint/4293/1/NPH%20Nam_MSCE_2020.pdf
[36] P.J. Goutam, D.K. Singh, and P.K. Iyer, "Photoluminescence quenching of poly (3-hexylthiophene) by carbon nanotubes," The Journal of Physical Chemistry C, **116**(14), 8196-8201 (2012). https://doi.org/10.1021/jp300115q
[37] D. Hernández-Martínez, et al., "Elaboration and characterization of P3HT–PEO–SWCNT fibers by electrospinning technique," SN Applied Sciences, **2**, 462-470 (2020). https://doi.org/10.1007/s42452-020-2278-2
[38] B.K. Kuila, S. Malik, S.K. Batabyal, and A.K. Nandi, "In-situ synthesis of soluble poly (3-hexylthiophene)/multiwalled carbon nanotube composite: Morphology, structure, and conductivity," Macromolecules, **40**(2), 278-287 (2007). https://doi.org/10.1021/ma061548e
[39] D. Meng, J. Sun, S. Jiang, Y. Zeng, Y. Li, S. Yan, J. Geng, and Y. Huanga, "Grafting P3HT brushes on GO sheets: distinctive properties of the GO/P3HT composites due to different grafting approaches," Journal of Materials Chemistry, **22**(40), 21583-21591 (2012). https://doi.org/10.1039/C2JM35317B
[40] V. Saini, Z. Li, S. Bourdo, E. Dervishi, Y. Xu, X. Ma, V.P. Kunets, "Electrical, optical, and morphological properties of P3HT-MWNT nanocomposites prepared by in situ polymerization." The Journal of Physical Chemistry C, **113**(19), 8023-8029 (2009). https://doi.org/10.1021/jp809479a
[41] H. Tai, X. Li, Y. Jiang, G. Xie, and X. Du, "The enhanced formaldehyde-sensing properties of P3HT-ZnO hybrid thin film OTFT sensor and further insight into its stability," Sensors, **15**(1), 2086-2103 (2015). https://doi.org/10.3390/s150102086
[42] J. Arranz-Andrés, and W.J. Blau, "Enhanced device performance using different carbon nanotube types in polymer photovoltaic devices," Carbon, **46**(15), 2067-2075 (2008). https://doi.org/10.1016/j.carbon.2008.08.027

СИНТЕЗ, ХАРАКТЕРИСТИКА ТА ФУНКЦІОНАЛІЗАЦІЯ НАНОКОМПОЗИТНИХ ПЛІВОК P3HT-CNT ЛЕГОВАНИХ Ag_2O

Хайдер Абдулмір Аббас[a], Віссем Шейкроху Кубаа[b], Естабрак Таліб Абдуллах[c]

[a]*Середній технічний університет, Інститут підготовки технічних інструкторів, Багдад, Ірак*

[b]*Університет Сфакс, Факультет природничих наук, Сфакс, Туніс*

[c]*Науковий коледж Багдадського університету, факультет фізики, Ірак*

Дослідження зосереджено на синтезі вуглецевих нанотрубок (CNT) і полі(3-гексилтіофену) (P3HT) (первинного полімеру) з легованими Ag (CNT/P3HT@Ag) нанокомпозитними тонкими плівками, для практичних застосувань. Були підготовлені чотири зразки розчину CNT з різним співвідношення полімеру (P3HT) [0,1, 0,3, 0,5 і 0,7 мас.%] для формування тонкого шару нанокомпозитів P3HT@CNT методом покриття Ag. Для дослідження властивостей поглинання та провідності для використання в різних практичних застосуваннях, у цьому дослідженні систематично оцінювалися структура, морфологія, оптичні та фотолюмінесцентні властивості нанокомпозиту CNT/P3HT@Ag. У зв'язку з цим використовувався спектрофотометр UV/Vis/NIR в діапазоні довжин хвиль від 350 до 700 нм для дослідження спектру поглинання, пропускання, коефіцієнта екстинкції (k) і показника заломлення зразків, виготовлених при кімнатній температурі. Результати XRD вказують на невелике збільшення розміру кристалітів синтезованого нанокомпозиту (CNT/P3HT@Ag) порівняно з нанокомпозитом CNT/P3HT, що можна пояснити кращою дисперсією P3HT та його сприятливим обгортанням навколо структур вуглецевих нанотрубок. Результати FESEM показують, що наночастинки Ag діють як місток між CNT і P3HT, створюючи зв'язок між двома матеріалами, який є достатньо міцним, щоб утворювати більш товсті трубчасті структури. Помітне збільшення інтенсивності поглинання (на приблизно 552 нм) досягається шляхом додавання наночастинок срібла до матриці CNT/P3HT при 0,5% P3HT. Крім того, підготовлені тонкі плівки CNT/P3HT@Ag демонструють більший коефіцієнт пропускання – понад 42%, 45%, 49% і 48% для концентрацій P3HT 1%, 3%, 5% і 7% відповідно. Підготовка даних про коефіцієнт екстинкції (k) і показник заломлення показує, що включення наночастинок срібла до нанокомпозитної матриці CNT/P3HT має значне покращення порівняно з попередніми зразками (композит CNT/P3HT).

Ключові слова: *нанокомпозит; полі(3-гексилтіофен) (P3HT); розчин вуглецевих нанотрубок (CNT); метод занурення; фотолюмінесцентні властивості; спектр пропускання*